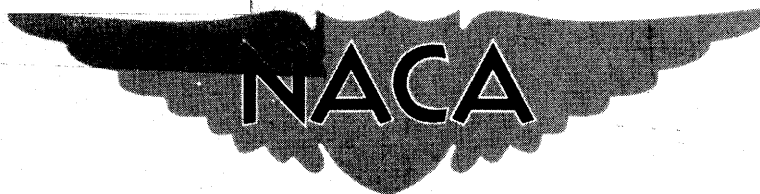




3 1176 00114 0061

c. 2



# RESEARCH MEMORANDUM

A SUMMARY OF NACA RESEARCH ON THE STRENGTH AND CREEP  
OF AIRCRAFT STRUCTURES AT ELEVATED TEMPERATURES

By Richard R. Heldenfels and Eldon E. Mathauser

Langley Aeronautical Laboratory  
Langley Field, Va.

CLASSIFICATION CHANGED

UNCLASSIFIED

To \_\_\_\_\_

NACA Re also

effective

By authority of FRN-126

Date Apr. 15, 1958

AMTS-12-58

CLASSIFIED DOCUMENT

This material contains information affecting the National Defense of the United States within the meaning of the espionage laws, Title 18, U.S.C., Secs. 793 and 794, the transmission or revelation of which in any manner to an unauthorized person is prohibited by law.

## NATIONAL ADVISORY COMMITTEE FOR AERONAUTICS

WASHINGTON

May 31, 1956

~~CONFIDENTIAL~~

~~CONFIDENTIAL~~

## NATIONAL ADVISORY COMMITTEE FOR AERONAUTICS

## RESEARCH MEMORANDUM

A SUMMARY OF NACA RESEARCH ON THE STRENGTH AND CREEP  
OF AIRCRAFT STRUCTURES AT ELEVATED TEMPERATURES<sup>1</sup>

By Richard R. Heldenfels and Eldon E. Mathauser

## SUMMARY

This paper summarizes some NACA research on the strength and creep of aircraft structural elements and components at elevated temperatures. Experimental data for aluminum-alloy columns, plates, stiffened panels, and multiweb box beams are presented for temperatures up to 600° F and compared with results predicted from materials data. Methods are described for predicting maximum strength from material stress-strain curves and creep lifetime from isochronous stress-strain curves. Some observations on the probable effect of creep on the design of aircraft structures are also included to illustrate the influence of design criteria on the weight of aircraft structures at elevated temperatures.

## INTRODUCTION

One of the most obvious and probably the most important of the many structural problems resulting from aerodynamic heating is the deterioration of material properties at elevated temperatures. This deterioration of material properties is reflected in loss of strength and creep of structures and can lead to weight increases that adversely affect the performance of high-speed aircraft. Consequently, the National Advisory Committee for Aeronautics has been investigating the strength and creep behavior of aircraft structural elements and components at elevated temperatures in order to obtain methods for predicting structural behavior from material characteristics. This paper presents the results of several experimental programs and indicates the accuracy with which these results can be predicted from basic materials data. Some observations on the probable effects of creep on aircraft structural design are also included.

---

<sup>1</sup>Presented at Symposium on High-Speed Aerodynamics and Structures sponsored jointly by Air Research and Development Command, Bell Aircraft Corporation, Cornell Aeronautical Laboratory, and University of Buffalo, January 18-20, 1956, at Buffalo, New York.

~~CONFIDENTIAL~~

## SYMBOLS

$b$	width, in.
$E_s$	secant modulus, ksi
$L$	length, in.
$n$	load factor
$n_L$	limit load factor
$t$	thickness, in.
$T_R$	temperature, °R
$\rho$	radius of gyration, in.
$\bar{\sigma}_f$	average stress at maximum load, ksi
$\sigma_{cy}$	0.2-percent-offset compressive yield stress, ksi
$\tau_f$	failure time, hr.

## EXPERIMENTAL INVESTIGATIONS

Experimental investigations were made to determine elevated-temperature strength and creep lifetime of columns, plates, stiffened panels, and multiweb box beams (refs. 1 to 4). These structural elements and components were constructed of aluminum alloy and were tested at temperatures ranging from room temperature to 600° F. In the tests to determine maximum strength, the structure was heated to test temperature and then loaded to failure. In the creep tests the structure was heated to test temperature and then exposed to load and temperature until failure occurred.

In discussing the results of these tests, experimental data from strength tests for each type of structural element are presented first and compared with predictions made with the aid of the material stress-strain curves. Then, creep lifetime results are presented and compared with predictions made from isochronous stress-strain curves. Finally, a brief discussion is made of the methods used to predict both maximum strength and creep lifetime. The type of materials data used in conjunction with these methods is illustrated in figure 1 where stress is plotted

against strain. The dashed line gives the stress-strain curve for 2024-T3 aluminum alloy at 400° F. The solid lines indicate isochronous stress-strain curves (ref. 5) that are defined in this paper as curves obtained by cross-plotting material compressive creep data to give stress as a function of strain for various lengths of exposure to load and temperature. These isochronous stress-strain curves were obtained from creep tests of plates of small width-thickness ratio supported in V-groove fixtures. The tick marks indicate the 0.2-percent-offset yield stresses.

Some exploratory tests were made to investigate the effect of intermittent heating and loading on creep lifetime of columns and to investigate the effect of creep on the maximum strength of plates. No methods, however, are available at the present time for predicting structural behavior for such conditions.

### Columns

Strength.- The results of tests to determine elevated-temperature strength of pin-ended 7075-T6 aluminum-alloy columns of solid rectangular cross section are shown in figure 2. (See ref. 1.) Stress is plotted against slenderness ratio for temperatures ranging from 300° F to 600° F. Test results are indicated by the symbols and predicted strengths are shown by the solid and dashed curves. In the elastic column range, shown by the dashed curves, the maximum strength of the columns was predicted from the Euler column formula by using the elastic modulus. In the inelastic column range, indicated by the solid curves, the maximum strength was predicted by substituting tangent moduli from material compressive stress-strain curves into the Euler column formula. A comparison between the experimental and predicted results indicates that this method satisfactorily predicts maximum strength of columns of all slenderness ratios at elevated temperatures.

Creep.- Creep tests were made at temperatures of 300° F, 400° F, 500° F, and 600° F; the results for 400° F are shown in figure 3 where stress is plotted against column lifetime for slenderness ratios ranging from 30 to 100. Predicted lifetimes obtained by substituting tangent moduli from isochronous stress-strain curves into the Euler column formula are indicated by the curves. Satisfactory agreement was obtained between the predicted and experimental results at 400° F and also at 500° F; however, agreement at other test temperatures has not yet been checked. Although the method used here for predicting lifetime does not establish the effect of initial out-of-straightness on column lifetime, it appears that a satisfactory approximation for lifetime of columns with small random initial out-of-straightness can thus be obtained. Lifetimes predicted by this method for columns with small initial out-of-straightness are in better agreement with experimental data than lifetimes determined from more elaborate theories available in the literature at the present time.

Creep tests with intermittent load and temperature.-- A few exploratory tests of columns subjected to intermittent temperature and load were made and the results are shown in figure 4. Lifetime ratio is plotted against temperature for slenderness ratios of 30, 50, and 70 for 7075-T6 aluminum-alloy columns similar to those previously discussed for continuous tests. The lifetime ratio is defined as the ratio of column lifetime obtained from the intermittent tests to lifetime obtained in the continuous tests for identical columns subjected to the same loads. The dashed line shown for a lifetime ratio of 1.0 indicates lifetime obtained from column creep tests in which load and temperature were maintained constant until collapse occurred. The lifetimes for these continuous tests ranged from 50 to 100 minutes. Experimental results obtained from tests of columns exposed to load and temperature for 10-minute periods until collapse occurred are indicated by the symbols where each symbol is the average of up to five tests. The total time during which the columns were subjected to both load and temperature until failure occurred is defined as the failure time in the intermittent creep tests. A lifetime ratio less than 1.0 was obtained in most of the intermittent tests; that is, the lifetime of the intermittently heated and loaded columns was less than the lifetime obtained from similar columns subjected to constant load and temperature. The results indicate that no simple cumulative creep effects are obtained from tests of this type.

Summary of column results.-- The results indicate that maximum strength of columns at any temperature can be estimated satisfactorily by using material compressive stress-strain data and the Euler column formula. Compressive creep data in the form of isochronous stress-strain curves appear to yield a satisfactory approximation for lifetime of columns with small random initial out-of-straightness; however, additional studies are needed to determine whether such a method will be generally successful. The data obtained from creep tests with intermittent load and temperature indicate that no simple cumulative creep effects are obtained from tests of this type.

### Plates

Strength.-- The results of experimental studies to determine maximum strength and creep lifetime of 2024-T3 aluminum-alloy plates at elevated temperatures are presented. (See ref. 2.) All plates were long with respect to their width and were tested with the unloaded edges supported in V-grooves. This type of support was used because maximum compressive strengths obtained from such plates at room temperature were found to agree well with strengths obtained from stiffened-panel and multiweb-box-beam tests.

Results from the strength tests of the 2024-T3 aluminum-alloy plates are shown in figure 5 where average stress at maximum load is plotted

against temperature. Experimental data are shown for width-thickness ratios from 20 to 60 and for temperatures up to 600° F. These experimental results apply to plates exposed to test temperature for 1/2 hour prior to strength testing. The maximum loads for plates with width-thickness ratios equal to 20 and 30 were approximately equal to the buckling load; for width-thickness ratios of 45 and 60, the maximum loads were substantially higher than the buckling loads. The increase in compressive strength produced by artificial aging of the aluminum alloy accounts for the predicted increased strength of the plates in the vicinity of 400° F. The predicted maximum strengths indicated by the curves are in good agreement generally with the experimental data.

The predicted maximum strengths were obtained by using a material parameter indicative of the overall shape of the material compressive stress-strain curve (ref. 6). The material parameter is defined as  $\sqrt{E_s \sigma_{cy}}$  where  $E_s$  is the secant modulus evaluated from the material compressive stress-strain curve at the maximum stress  $\bar{\sigma}_f$ , and  $\sigma_{cy}$  is the 0.2-percent-offset compressive yield stress. Plate-test results for several materials and temperatures are plotted in terms of this parameter in figure 6. The average stress at maximum load  $\bar{\sigma}_f$  divided by the material parameter  $\sqrt{E_s \sigma_{cy}}$  is plotted against the plate thickness-width ratio  $t/b$ . The plate-test results shown previously in figure 5 are indicated by the open symbols. The solid symbols indicate room-temperature results for plates of magnesium alloy, three aluminum alloys, and stainless steel. All results at room and elevated temperature lie essentially along a straight line and indicate that the maximum strength of the plates can be obtained from the equation defining the straight line on this plot. The material parameter  $\sqrt{E_s \sigma_{cy}}$  is thus useful for predicting maximum strength of plates at any temperature. Plate strengths determined in this manner agree closely with experimental plate strengths obtained from stiffened-panel and multiweb-box-beam tests.

**Creep.** Creep test results for 2024-T3 aluminum-alloy plates at 400° F are given in figure 7 where stress is plotted against lifetime. Experimental results indicated by the symbols are shown for width-thickness ratios ranging from 20 to 60. Predicted lifetimes shown by the curves were obtained by using material compressive creep data in the form of isochronous stress-strain curves and the material parameter  $\sqrt{E_s \sigma_{cy}}$  in a manner analogous to the determination of maximum plate strength. This method appears to yield a satisfactory approximation for plate lifetime because the agreement between the experimental data and predicted results is satisfactory. Similar agreement between experimental and predicted lifetimes was obtained at 450° F and 500° F for plates of the same material (ref. 2).

For the plate-creep results shown, the applied stresses were less than the predicted buckling stresses for width-thickness ratios of 20 and 30.

During the tests buckles appeared gradually and continued to increase in depth until collapse occurred. For width-thickness ratios of 45 and 60, buckles were obtained immediately upon loading in all but one plate specimen. The buckles gradually increased in depth during the creep tests until collapse occurred.

The lifetime results for plates of one material at many temperatures can be summarized on one plot as shown in figure 8. Stress is plotted against the Larson-Miller time-temperature parameter  $T_R(17 + \log \tau_f)$  (ref. 7) often used to summarize tensile creep data. In this parameter,  $T_R$  is the absolute temperature in degrees Rankine, 17 is a material constant, and  $\tau_f$  is lifetime in hours. Plate-creep data are shown for several width-thickness ratios from 20 to 60 and for temperatures of 400° F, 450° F, and 500° F. Tensile creep rupture data are shown by the line symbols for temperatures of 375° F, 400° F, and 450° F. The dashed curve indicates an average of the tensile rupture data. These results indicate that creep data from tests of both structural components and materials can be plotted in terms of a time-temperature parameter. Data in this form are convenient for estimating combinations of stress, temperature, and time that produce creep failure. For the results shown here, note that the lifetime data for plates of width-thickness ratio of 20 lie close to the tensile rupture curve. This result indicates that a plate of  $b/t = 20$  will support a given stress, either tensile or compressive, for approximately the same length of time. For larger  $b/t$ , the plates will fail sooner in compression than in tension.

Effect of creep on maximum strength of plates.- In order to explore the effect of creep on the strength of plates, some 2024-T3 aluminum-alloy plates similar to those previously discussed were tested in combination creep and strength tests. A typical result from such tests is shown in figure 9 where stress is plotted against unit shortening for three plates tested at 400° F. The solid curve is a plot of stress against unit shortening obtained in the strength test of the plate after 6-hours exposure to temperature. The dot-dash curve shows the creep-test result for a similar plate loaded at a stress equal to approximately 80 percent of the maximum strength of the plate after 6-hours exposure. The unit shortening at failure which occurred in 8.4 hours is indicated by the circular symbol and the tick marks indicate unit shortening at 2-hour intervals in the creep tests. The dashed curve gives the result for a plate that was subjected to creep for 6 hours (65 percent of life) and then tested to ultimate strength. The strength of this plate was approximately the same as that obtained for the plate exposed to temperature for the same time. The results indicate that the primary effect of creep is to increase the unit shortening at maximum load by a magnitude approximately equal to the value of shortening obtained during the creep period prior to strength testing.

The results of figure 9 and some additional results are presented in a different manner in figure 10 where stress is plotted against time. The solid curves drawn through the circular and square symbols indicate maximum strength for various exposure times and creep lifetime, respectively. The maximum strengths were obtained by exposing the plates to test temperature for the time shown in the abscissa and then loading to maximum strength. The lifetime data were obtained by loading the plate to the stress shown in the ordinate and maintaining both load and test temperature until failure occurred. The combination creep and strength tests are indicated by the dashed lines. In these tests the plates were loaded at stress levels ranging from 67 percent to 80 percent of the maximum strength obtained for the plates that were exposed to test temperature for 6 hours. The maximum strengths obtained in the combination tests after 6 or 12 hours of creep are shown by the solid symbols. The results indicate that subjecting the plates to considerable creep prior to strength testing has little effect on maximum strength if the effect of exposure to elevated temperature is properly accounted for. These results for one plate width-thickness ratio at one temperature are typical of results obtained for other plate proportions ( $b/t = 30, 45, \text{ and } 60$ ) at  $400^{\circ}\text{ F}$  and  $500^{\circ}\text{ F}$ .

Summary of plate results.- The results from the strength tests indicate that the maximum compressive strength of plates supported in V-grooves can be predicted satisfactorily at any temperature by using the parameter  $\sqrt{E_s \sigma_{cy}}$  determined from the material compressive stress-strain curve. Creep lifetime appears to be predicted satisfactorily in an analogous manner by substituting compressive creep data in the form of isochronous stress-strain curves for the material stress-strain curves. In addition, creep lifetime obtained experimentally at several temperatures for plates of one material can be summarized in one plot by using the Larson-Miller time-temperature parameter  $T_R(17 + \log \tau_f)$  often used to summarize tensile creep rupture results. Data obtained from combination creep and strength tests indicate that subjecting the plates to considerable creep prior to strength testing has little effect on maximum strength if the effect of exposure to elevated temperature is properly accounted for.

### Stiffened Panels

Strength.- The results of some exploratory tests to determine elevated-temperature strength and creep lifetime of stiffened panels are presented. Tests were made on 2024-T aluminum-alloy panels of identical cross section and four different lengths (ref. 3). The panels were tested flat-ended and an end-fixity coefficient of 3.75 was used to reduce the test data. Strength-test results are given in figure 11 where stress is plotted against slenderness ratio for stiffened panels of the indicated cross section. Test results at room temperature and  $400^{\circ}\text{ F}$  are shown by the symbols; predicted results, by the curves. Euler buckling stresses



for the panels at room temperature and 400° F are also shown. Column strength of the panels was determined by using the load-shortening curve from the shortest panel as an "effective" stress-strain curve. The slopes from the load-shortening curve were substituted into the Euler column formula. The load-shortening curve for the short panel may be obtained experimentally or may be approximated from materials data and a load-shortening curve from a panel of identical geometry of different material (ref. 8). The maximum or crippling strength of short panels can be estimated by summing the calculated strengths of the plate elements of the panel. The method discussed previously for estimating maximum plate strength can be used for this purpose.

Creep. - Creep-test results obtained from stiffened panels identical in construction to those described in the strength tests are shown in figure 12. Stress is plotted against lifetime. Experimental results obtained at 400° F for slenderness ratios from 18 to 92 are given by the symbols. The lines indicate lifetimes predicted from isochronous load-shortening curves. These curves were approximated from isochronous stress-strain curves and an experimental load-shortening curve from a strength test of a short panel (ref. 3). The predicted results are in satisfactory agreement with the experimental data for the short panels, but for the longer panels the predicted results are conservative. For the experimental results shown here, buckles were produced in the skin of all panels immediately upon loading. The buckles increased in depth during the tests and were accompanied by lateral deflection of the stiffeners until collapse occurred.

Summary of stiffened-panel results. - The limited experimental data at elevated temperatures on stiffened panels indicate that column strength can be estimated with the aid of the load-shortening curve from a short panel and the Euler column formula. The maximum or crippling strength of short panels can be predicted satisfactorily by summing the calculated strength of the plate elements of the panel. Creep lifetime can be estimated from methods used to predict maximum strength by substituting isochronous stress-strain curves for material stress-strain curves. The predicted lifetimes are in satisfactory agreement for the shorter panels and appear to be conservative for the long panels.

#### Multiweb Box Beams

Strength. - A few tests were made to determine elevated-temperature maximum strength and creep lifetime of aluminum-alloy multiweb box beams of one cross section. (See ref. 4.) These strength-test results are summarized in figure 13 where stress is plotted against temperature for different exposure times. The ultimate tensile strength of 2024-T3 aluminum alloy for 1/2-hour and 2-hour exposure time prior to loading is shown

by the solid curves. The dashed curves indicate the maximum compressive strength of the box-beam cover plates for the indicated exposure times. A symmetrically designed multiweb box beam, that is, a beam with equal-thickness cover plates, is expected to fail in compression throughout the temperature range shown for 1/2-hour exposure. The experimental strengths indicated by the square symbols are in agreement with this prediction. For 2-hours exposure, compression failure was predicted for all temperatures except in the range from 375° F to 475° F. In this temperature range, tensile failure was predicted and was verified experimentally as shown by the circular symbol.

Creep.- Results were obtained from creep tests of three multiweb box beams. The correlation between these results and tensile-rupture and plate-creep data is indicated in figure 14. Stress is plotted against the Larson-Miller time-temperature parameter  $T_R(17 + \log \tau_f)$  shown previously in conjunction with creep-test results for plates. Data obtained from the multiweb-box-beam creep tests are indicated as follows: tensile failure by the circles, and compressive failure by the square. Failure time and test temperature for each beam are indicated in the key. The tension and compression covers of these beams were made of 1/8-inch-thick 2024-T3 aluminum-alloy sheet and had width-thickness ratios between webs of 20. The beams were subjected to constant loads at elevated temperatures until failure occurred. The region between the dashed curves indicated by vertical lines shows the limits of scatter for tensile-creep-rupture data. The region between the solid curves indicated by horizontal lines shows the limits of scatter for creep-lifetime data from plates of width-thickness ratio of 20. The box-beam results agree favorably with the plate and tensile-rupture data. The results indicate that aluminum-alloy multiweb box beams having equal-thickness cover plates with width-thickness proportions of 20 are of nearly balanced design in the temperature range investigated; that is, the tension and compression covers are approximately equally resistant to creep failure.

Summary of multiweb-box-beam results.- The elevated-temperature tests of multiweb box beams indicate that maximum strength can be predicted by using elevated-temperature tensile and compressive stress-strain data in conjunction with methods used for determining room-temperature strength. It appears that creep lifetime can be estimated satisfactorily from tensile-rupture and plate-creep data; however, additional tests are needed to verify this assumption.

#### EFFECT OF CREEP ON AIRCRAFT STRUCTURAL DESIGN

The preceding discussion of the creep of structural components was concerned with creep behavior of these members when subjected to stresses

large enough to produce significant creep. The question as to whether creep will be important in the design of aircraft structures obviously depends upon the magnitude and time duration of the loads and temperatures encountered by the aircraft. Some data on the load experience of aircraft are combined with materials data to obtain indications of the effect of creep on aircraft structural design in much the same manner as in references 9 and 10. Some data on the magnitude and duration of the loads encountered by airplanes are presented in figure 15. The relationship between load and time typical of present-day airplanes is indicated by the load ratio  $n/n_L$  plotted against the percentage of total flight time spent above that load ratio. The load ratio is the actual load  $n$  divided by the design limit load  $n_L$ . The solid line is for a fighter-type airplane and the dashed line for a bomber type. Figure 15 was prepared from existing gust-loads data (ref. 11) and maneuver-loads data (ref. 12). The time spent at the low load ratios for each type is primarily due to gusts and that at the higher loads is primarily due to maneuvers. Note that percent time is plotted on a logarithmic scale and that most of the total time is spent at low load ratios, about 90 percent of the time for the fighter and 99.9 percent for the bomber.

The foregoing load-time relations are representative of airplanes in flight at speeds below sonic. Similar relations for supersonic airplanes have not been established, but it seems reasonable to assume that the load-time relations will not be substantially different from those shown in figure 15. The significance of these data is that high-speed airplanes will spend a very small percentage of their lifetime at loads near the design limit load where creep is most likely to be important. In addition, these high loads will not necessarily occur in conjunction with high temperatures.

The uncertainties that exist in the expected loads and the limited data available on cyclic and intermittent creep make a detailed analysis of the effects of creep on structural weight impracticable at present; however, in the present paper some approximate indications of the weight of tensile members are obtained by assuming various creep and strength criteria.

In order to obtain a creep design criterion, the assumption is made that all loads can be represented by only two levels, a low level representative of most of the flight time (for example, about 0.2 load ratio for 90 percent of the life of the fighter) and that the remaining percent of the lifetime is spent at a second level, the design limit load. It can be shown that the lower load level makes an insignificant contribution to the creep of the tensile member and can thus be neglected in the analysis. Despite large differences in the load experience and expected service life, similar final results are obtained for both fighters and bombers; therefore, for this paper, the analysis is restricted to fighters. The total time that the fighter spends at elevated temperature is conservatively estimated to be 1,000 hours, of which 100 hours or 10 percent is spent at limit load. The creep design criterion is taken as creep rupture in 100 hours at limit load and the weight required for this creep criteria is compared with two strength criteria.

The first comparison is given in figure 16 where the weight in arbitrary units is plotted against temperature for four materials: 2024-T3 aluminum alloy, RC-130A titanium alloy, 17-7 PH stainless steel, and Inconel X. The dashed curves indicate the weight of the tensile member which will support limit load for 100 hours before tensile rupture will occur. The solid curves indicate the weight required for a tensile member that has an ultimate strength  $1\frac{1}{2}$  times the limit load after

1,000-hours exposure to temperature. On the basis of these creep and strength criteria, the aluminum-alloy tensile member requires less weight for creep than for strength. Similar results are obtained for the titanium alloy up to 500° F, for the stainless steel up to 900° F, and for Inconel X up to 1200° F. Above these temperatures for the respective materials, the design on the basis of creep requires more weight than the design for strength. Note that, above the temperature where the creep criterion determines the weight required, design efficiency is improved by conversion to the next material and the creep problem is avoided. However, conversion to different materials at the high temperatures may not always be practical and creep may well become a primary design factor at high temperatures where all commonly available structural materials experience significant creep.

A second comparison is made by using as the strength criterion the yield strength equal to the limit load after 1,000-hours exposure to temperature; the creep criterion is not changed. The results of this analysis are given in figure 17 where weight, again in arbitrary units, is plotted against temperature for the four materials shown in figure 16. The solid curves indicate the weight of a tensile member that has a yield strength equal to the limit load after 1,000-hours exposure to temperature. The dashed curves indicate the weight of the tensile member that will support limit load for 100 hours before creep rupture occurs. For the aluminum alloy the creep criterion requires less weight up to about 325° F, but beyond this temperature the two criteria require approximately equal weights. For the titanium alloy and stainless steel the design for creep requires more weight than the design for yield strength. A similar result is obtained for Inconel X above 1,200° F. A comparison of figures 16 and 17 indicates that creep has more influence on the design when the yield strength criterion is used. Similar differences also appear if the creep criterion is changed; for example, reducing rupture time from 100 to 10 hours moves the dashed curves to the right and decreases the significance of creep as may be expected. The 100-hour creep criterion used in this analysis is believed to be a very conservative one.

The effect of creep on aircraft structural design is thus greatly dependent on the design criterion used. Creep rupture in a specified time was used in this analysis because of its obvious significance and the general availability of such data. A prescribed amount of permanent creep strain or deformation or a limiting amount of total deformation might have been used, but the validity of a general criterion of this type appears

doubtful. Although a maximum deformation can be established for a particular structure, a reasonable limiting strain of general significance could not be established from the measured deformations of the structural elements and components discussed previously in this paper. If a strain or deformation criterion is not used as the design criterion, it may nevertheless be necessary to check some structures for excessive creep deformations.

These remarks on creep effects in aircraft structural design indicate that so many factors combine to determine the true influence of creep that no definite conclusions can be drawn at this time. It appears, however, that creep may well be a primary design criterion only at the high temperatures where all available materials exhibit substantial creep. Moreover, future high-speed aircraft will carry needless structural weight unless a realistic creep design criterion is established from studies of the expected load-temperature-time experience of each aircraft.

#### CONCLUDING REMARKS

This paper has presented the experimental results of NACA investigations to date on the strength and creep of aircraft structural components at elevated temperatures and approximate methods for predicting the experimental results have been described. These methods were usually satisfactory for predicting the experimental results from basic materials data; however, additional research is needed to establish the general applicability of the methods. Some observations on the probable effect of creep on aircraft structural design were also included to illustrate the influence of design criteria on the weight of aircraft structures at elevated temperature.

Langley Aeronautical Laboratory,  
National Advisory Committee for Aeronautics,  
Langley Field, Va., March 27, 1956.

## REFERENCES

1. Mathauser, Eldon E., and Brooks, William A., Jr.: An Investigation of the Creep Lifetime of 75S-T6 Aluminum-Alloy Columns. NACA TN 3204, 1954.
2. Mathauser, Eldon E., and Deveikis, William D.: Investigation of the Compressive Strength and Creep Lifetime of 2024-T3 Aluminum-Alloy Plates at Elevated Temperatures. NACA TN 3552, 1956. (Supersedes NACA RM L55E11b.)
3. Mathauser, Eldon E., and Deveikis, William D.: Investigation of the Compressive Strength and Creep Lifetime of 2024-T Aluminum-Alloy Skin-Stringer Panels at Elevated Temperatures. NACA TN 3647, 1956.
4. Mathauser, Eldon E.: Investigation of Static Strength and Creep Behavior of an Aluminum-Alloy Multiweb Box Beam at Elevated Temperatures. NACA TN 3310, 1954.
5. Shanley, F. R.: Weight-Strength Analysis of Aircraft Structures. McGraw-Hill Book Co., Inc., 1952, pp. 265-305.
6. Anderson, Roger A., and Anderson, Melvin S.: Correlation of Crippling Strength of Plate Structures With Material Properties. NACA TN 3600, 1956.
7. Larson, F. R., and Miller, James: A Time-Temperature Relationship for Rupture and Creep Stresses. Trans. A.S.M.E., vol. 74, no. 5, July 1952, pp. 765-771; Discussion, pp. 771-775.
8. Dow, Norris F., and Anderson, Roger A.: Prediction of Ultimate Strength of Skin-Stringer Panels From Load-Shortening Curves. Preprint no. 431, S.M.F. Fund Preprint, Inst. Aero. Sci., Jan. 1954.
9. Heldenfels, Richard R.: Some Design Implications of the Effects of Aerodynamic Heating. NACA RM L55F22, 1955.
10. Heldenfels, Richard R.: Some Elevated Temperature Structural Problems of High-Speed Aircraft. Preprint no. 599, SAE Golden Anniversary Aero. Meeting, Oct. 11-14, 1955.
11. Press, Harry, Meadows, May T., and Hadlock, Ivan: Estimates of Probability Distribution of Root-Mean-Square Gust Velocity of Atmospheric Turbulence From Operational Gust-Load Data by Random-Process Theory. NACA TN 3362, 1955.
12. Mayer, John P., and Hamer, Harold A.: A Study of Means for Rationalizing Airplane Design Loads. NACA RM L55E13a, 1955.

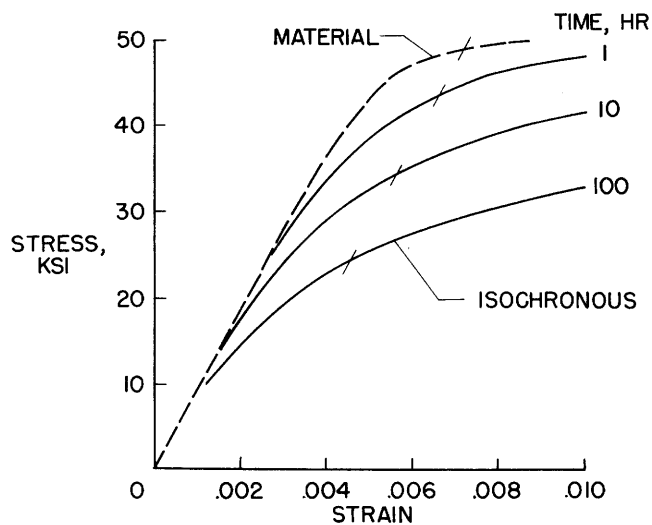


Figure 1.- Material and isochronous compressive stress-strain curves for 2024-T3 aluminum alloy at 400° F.

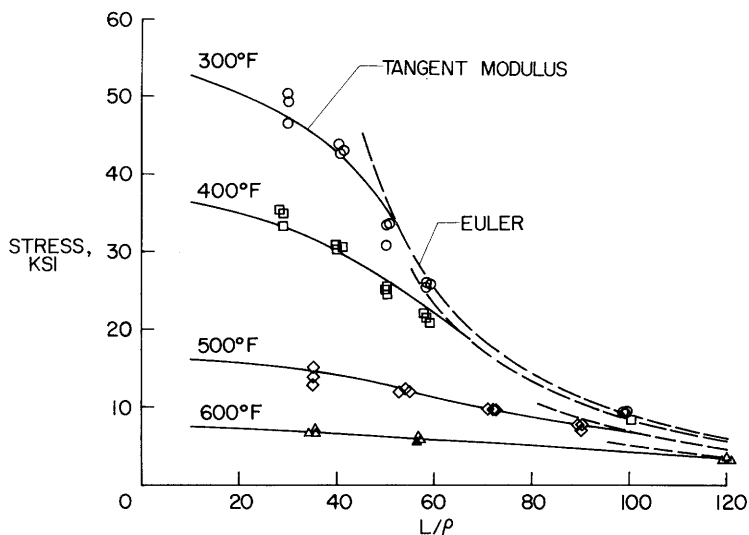


Figure 2.- Experimental and predicted maximum strengths of pin-ended 7075-T6 aluminum-alloy columns at elevated temperatures. 1/2-hour exposure.

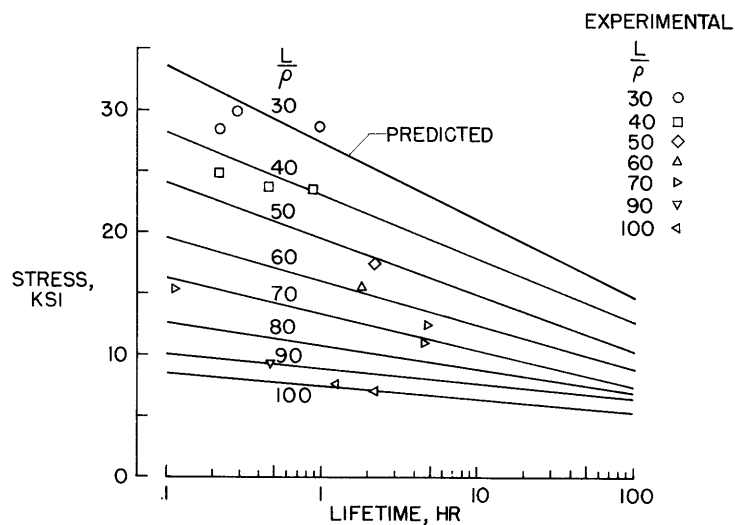


Figure 3.- Experimental and predicted lifetimes of 7075-T6 aluminum-alloy columns at 400° F.

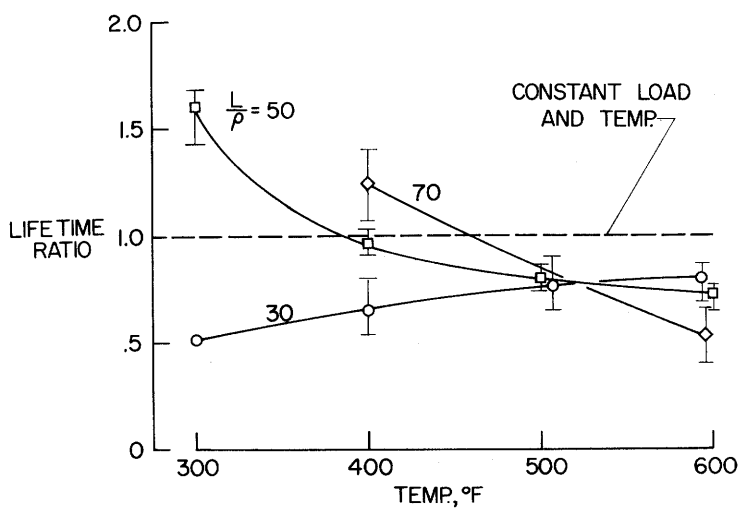


Figure 4.- Effect of intermittent heating and loading on lifetime of 7075-T6 aluminum-alloy columns at elevated temperatures.



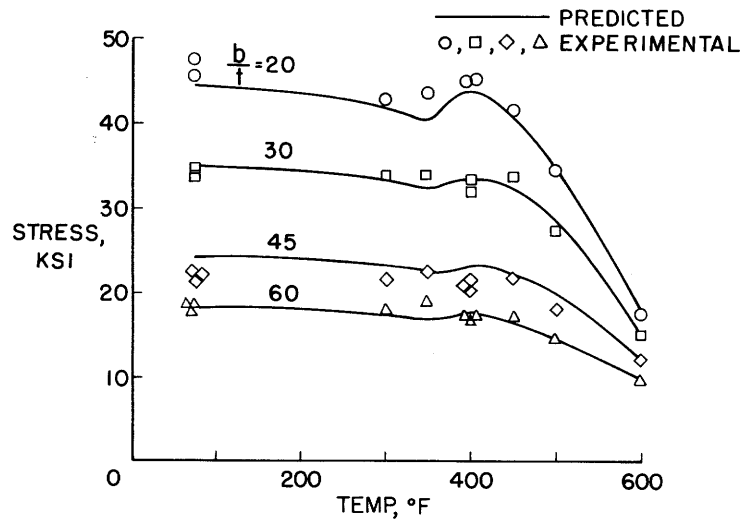


Figure 5.- Experimental and predicted compressive strengths of 2024-T3 aluminum-alloy plates. 1/2-hour exposure.

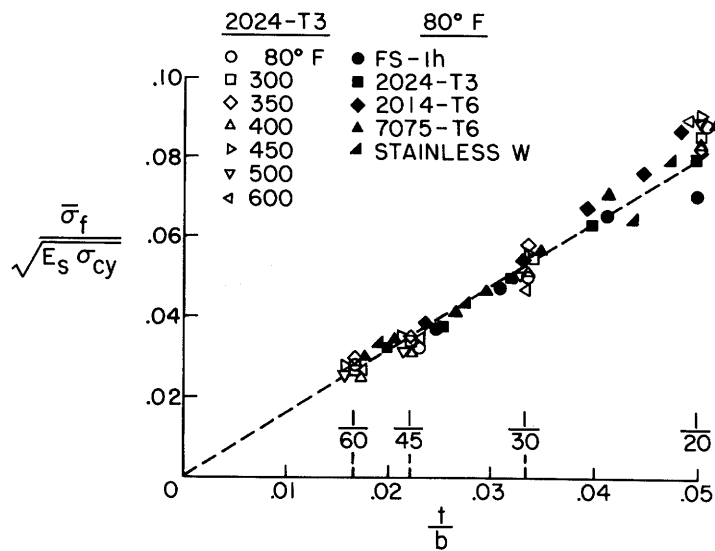


Figure 6.- Correlation of room- and elevated-temperature plate strengths with material properties.

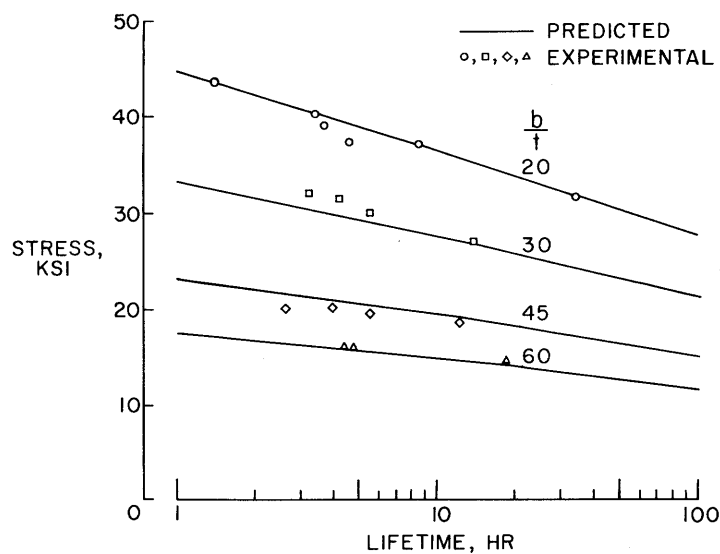


Figure 7.- Experimental and predicted lifetimes of 2024-T3 aluminum-alloy plates at 400° F.

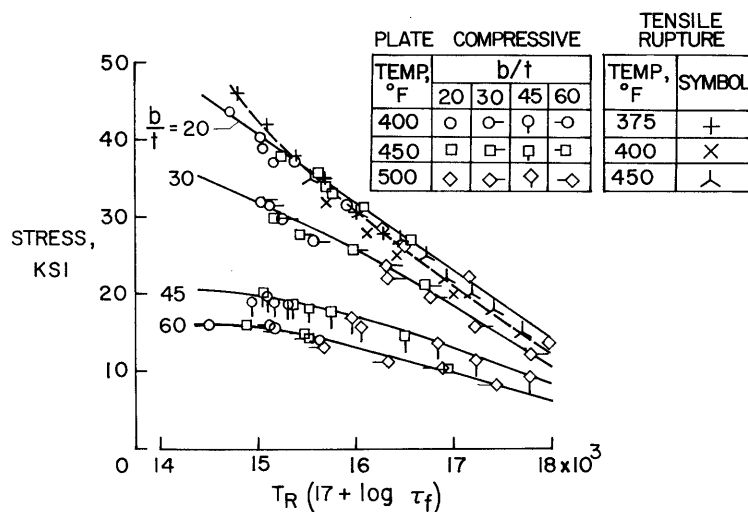


Figure 8.- Master creep lifetime curves for 2024-T3 aluminum-alloy plates.

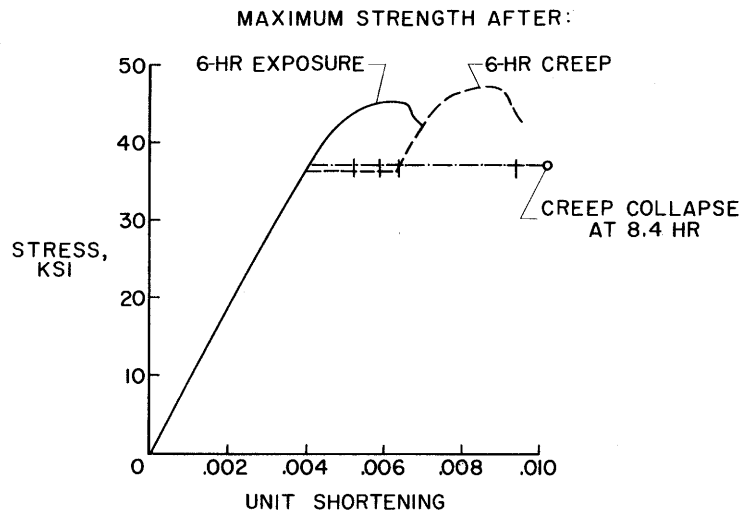


Figure 9.- Effect of exposure time and creep strain on the maximum strength and unit shortening of 2024-T3 aluminum-alloy plates at 400° F.  $b/t = 20$ .

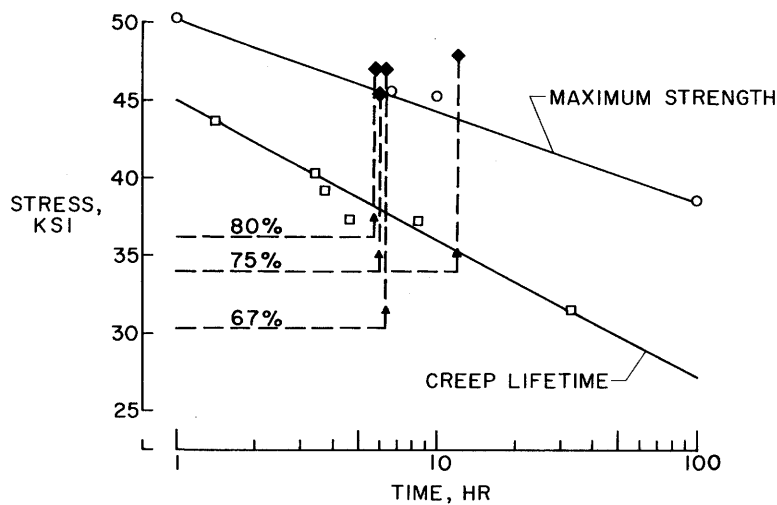


Figure 10.- Effect of creep strains on the maximum strength of 2024-T3 aluminum-alloy plates at 400° F.  $b/t = 20$ . Solid symbols are results from combination creep and strength tests.

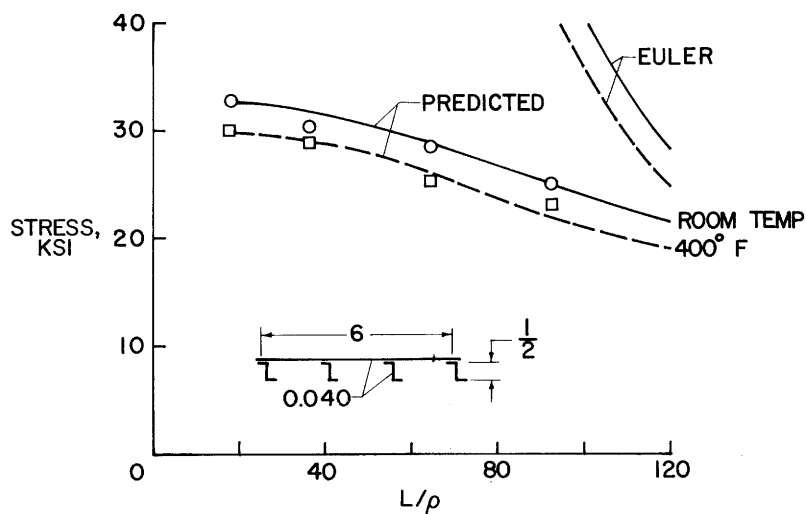


Figure 11.- Experimental and predicted maximum strengths of 2024-T aluminum-alloy skin-stringer panels.

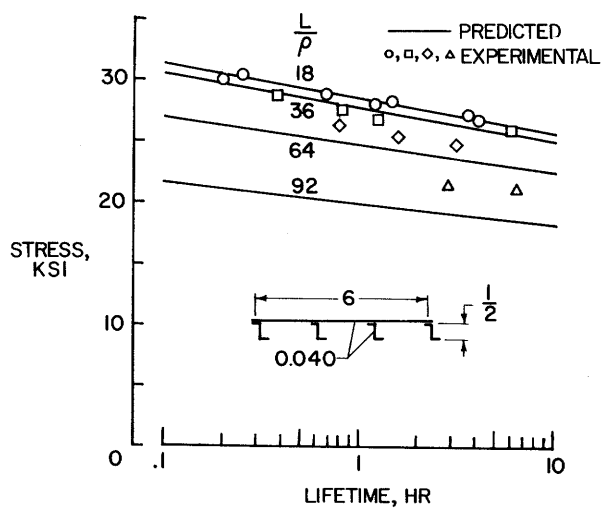


Figure 12.- Experimental and predicted lifetimes of 2024-T aluminum-alloy skin-stringer panels at 400°F.

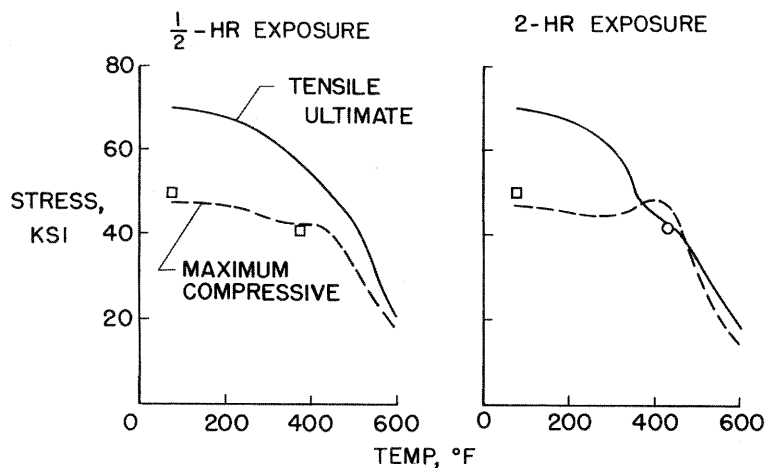


Figure 13.- Variations of ultimate tensile and maximum compressive stresses with temperature for 2024-T3 aluminum-alloy box beams; maximum strength test results indicated by symbols.

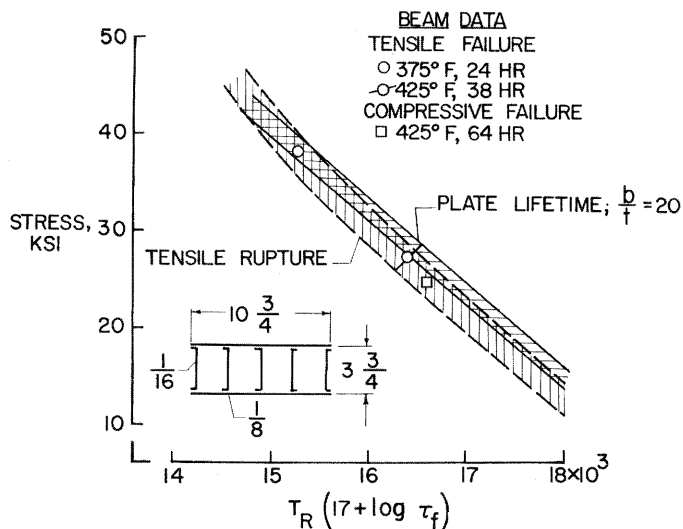


Figure 14.- Comparison of multiweb box beam lifetimes with tensile rupture and plate creep lifetime data. 2024-T3 aluminum alloy.

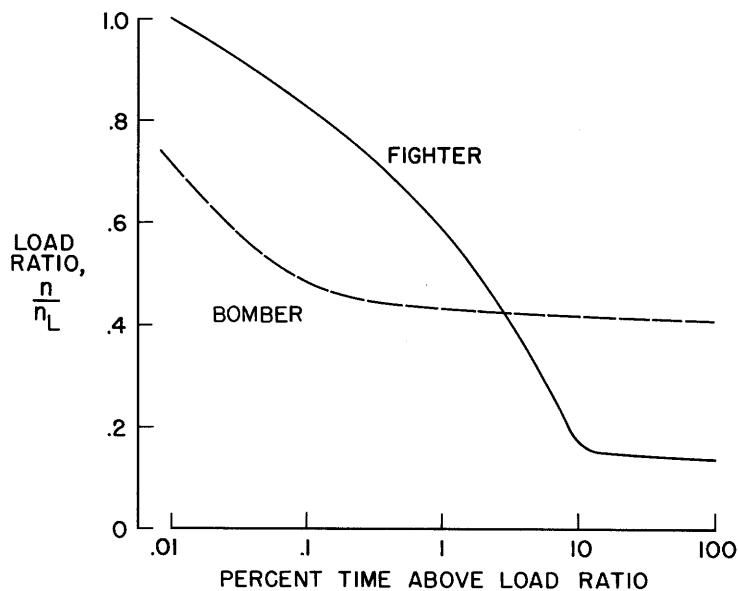


Figure 15.- Load-time relations for fighter- and bomber-type airplanes.

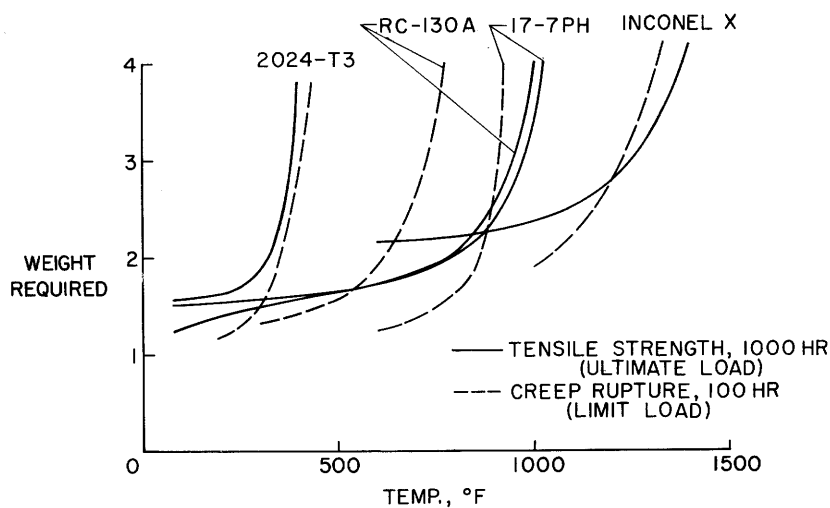


Figure 16.- Weight of four materials required to support equal tensile loads at elevated temperatures as determined by an ultimate strength and a creep-rupture criteria.

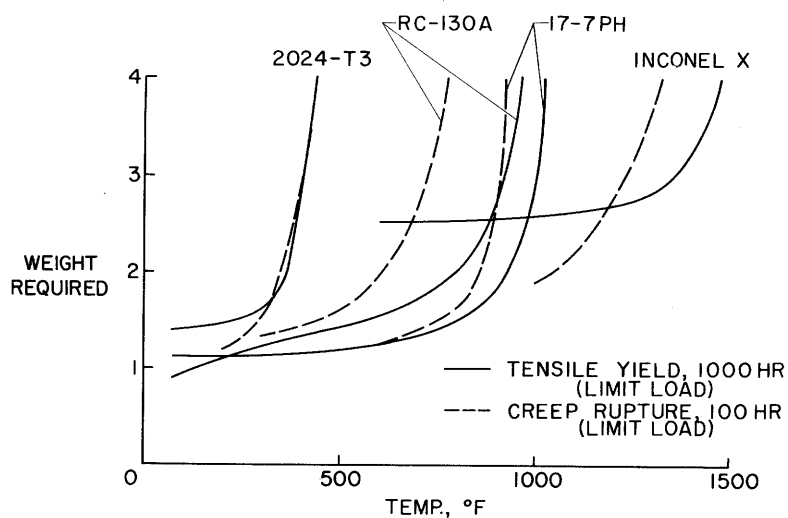


Figure 17.- Weight of four materials required to support equal tensile loads at elevated temperatures as determined by a yield strength and a creep-rupture criteria.